Replication of murine coronavirus requires multiple cysteines in the endodomain of spike protein

Jinhua Yang, Jun Lv, Yuyan Wang, Shuang Gao, Qianqian Yao, Di Qu, Rong Ye *

Shanghai Medical College, Fudan University, Shanghai 200032, China

ABSTRACT

A conserved cysteine-rich motif located between the transmembrane domain and the endodomain is essential for membrane fusion and assembly of coronavirus spike (S) protein. Here, we proved that three cysteines within the motif, but not dependent on position, are minimally required for the survival of the recombinant mouse hepatitis virus. When the carboxy termini with these mutated motifs of S proteins were respectively introduced into a heterogeneous protein, both incorporation into lipid rafts and S-palmitoylation of these recombinant proteins showed a similar quantity requirement to cysteine residues. Meanwhile, the redistribution of these proteins on cellular surface indicated that the absence of the positively charged rather than cysteine residues in the motif might lead the dramatic reduction in syncytial formation of some mutants with the deleted motifs. These results suggest that multiple cysteine as well as charged residues concurrently improves the membrane-associated functions of S protein in viral replication and cytopathogenesis.

© 2012 Elsevier Inc. All rights reserved.

Introduction

Coronaviruses are a family of enveloped, positive-sense RNA viruses that principally cause respiratory or enteric infections in humans and a broad range of animals (Holmes, 2003; Masters, 2006; Siddell, 1995). Mouse hepatitis virus (MHV), a member of the group II of coronaviruses (now called genus Betacoronavirus) (Carstens and Ball, 2009), causes neurovirulence and hepatitis in rodents, such as mice and rats (Weiss and Navas-Martin, 2005). MHV has been used extensively for in vivo studies of neurovirulence and mechanisms of coronavirus entry and assembly (Masters, 2006). Three membrane proteins, including the spike (S), envelope and membrane proteins, are incorporated into the envelope of MHV virions (Masters, 2006; Siddell, 1995). The S protein is a 180 kDa, N-glycosylated, type I membrane protein which is generally cleaved into separate N-terminal S1 and C-terminal S2 subunits. The main component of the S protein is the ectodomain (Ecto) in which a few functional domains have been clearly described. These include the receptor-binding domain from S1 as well as the fusion peptide and two heptad repeats (HR1 and HR2) from S2. The Ecto is responsible for the cellular tropism and membrane fusion in coronavirus infection (Masters, 2006; Siddell, 1995). The minor part of the S protein is composed of a transmembrane domain (Tm) and an endodomain (Endo).

There are up to ten highly conserved cysteine residues located between the Tm and the Endo of all coronavirus S proteins (Bos et al., 1995). Previous studies have revealed that the cysteine-rich (CR) motif of S proteins is essential for virion assembly and membrane fusion (Bos et al., 1995; Bosch et al., 2005; Chang et al., 2000; Lopez et al., 2008; Petit et al., 2007; Shulla and Gallagher, 2009; Thorp et al., 2006; Ye et al., 2004). We have found that a 13-residue deletion leaving only four to five cysteine residues in the motif reduced syncytia formation dramatically but did not distinctly affect the replication of recombinant MHVs in mouse L2 cells, suggesting that these residues in the motif play different roles in virion assembly and trafficking of the S protein to the plasma membrane (Yang et al., 2011; Ye et al., 2004).

S-palmitoylation is the covalent attachment of 16-C saturated fatty acids to cysteine residues of membrane proteins via a thioester linkage (Brown and London, 1998). This reversible modification can influence protein trafficking between membrane compartments and protein stability by adding fatty acid chains to proteins (Linder and Deschenes, 2007; Rocks et al., 2005). S-palmitoylation of coronavirus S protein is focused in the CR motif (Bos et al., 1995; Bosch et al., 2005; McBride and Machamer, 2010; Petit et al., 2007; Thorp et al., 2006). The modification also occurs on the cysteine residues in the cytoplasmic tails of other viral membrane proteins, such as influenza virus Hemagglutinin (Chen et al., 2005; Jin et al., 1996; Kordyukova et al., 2008; Takeda et al., 2003; Zhang et al., 2000), paramyxovirus F (Branigan et al., 2006), vesicular stomatitis virus G (Whitt and Rose, 1991), hepatitis C virus core (Majeau et al., 2009), HIV-1 envelope (Rousso et al., 2000), Sindbis virus E1 and E2 (Smit et al., 2001) and baculovirus gp64 (Zhang et al., 2003). This modification enables

* Corresponding author at: Shanghai Medical College, Fudan University, 138 Yixueyuan Road, P.O. Box 168, Shanghai 200032, China. Fax: +86 21 54237374.
E-mail address: yerong24@fudan.edu.cn (R. Ye).

the association of viral proteins with lipid rafts, which is essential for viral infectivity (McBride and Machamer, 2010; Zhang et al., 2000). However, the mechanism of S-palmitoylation on viral membrane proteins is not clearly understood.

In this study, the functional importance of the cysteine residues in the MHV S Endo for viral replication was investigated by reverse genetics. There was no single "key" cysteine residue required in the motif for virus replication. However, at least three cysteine residues were found to be required for the survival of recombinant MHVs. Immunofluorescence analysis of the heterogeneous hook proteins (HK) expressed by recombinant MHVs (Yang et al., 2011; Ye et al., 2004) showed that the dramatic reduction of the cytopathic effect (CPE) of recombinant MHVs with a partial deletion of motif did not involve these cysteines. This effect might result from the deletion of some of the charged residues in the motif, which decreased the amount of S protein on the surfaces of infected cells. Furthermore, both incorporation into detergent-resistant membrane fractions (DRM) and the S-palmitoylation level of these recombinant protein were examined. Results showed that an association into lipid rafts and S-palmitoylation of the recombinant protein with a deletion motif containing six cysteines not only was detected but also exhibited a similar level to that of wild-type motif. However, the protein with a deletion motif containing only two cysteines could not be detected.

Results

No single specific cysteine in the S protein endodomain was essential for virus replication

There are nine cysteines in the CR motif of the MHV S protein (Lopez et al., 2008). To examine the effects of these residues on virus replication, a series of recombinant MHVs was constructed with mutated S Endo by RNA targeted recombination (Fig. 1A). The deletion of all 18 residues of the CR motif (Mut-d1), the deletion of 10 residues of the CR motif near the Tm (Mut-d2), and the substitution of all nine cysteine residues of the CR motif with alanine residues (Mut-p1) were lethal for the respective recombinant MHVs (Fig. 1B).

However, the deletion of 8 residues in the CR motif near the Endo (Mut-d3) and all point mutations of 1–2 cysteine residues (Mut-p2 to -p7) did not impair the survival of recombinant MHVs (Fig. 1B). The size of plaques produced by all survived mutants was significantly smaller than that of the wild-type MHV (p<0.001) (Fig. 1C). The statistical analysis showed that the partial deletion mutant (Mut-d3) produced smaller plaques compared with other point mutants (Mut-p2 to -p7) that could be further divided into three groups from small to large: Mut-p4, -p5, and -p7; Mut-p2 and -p3; Mut-6. The tendency might be associated with the importance of these mutated cysteines in the motif. We observed that there was no significant difference between one and two cysteine substitution. Also, the substitution with alanine, serine, or glycine showed the similar effect. Notably, the boundary of the plaques formed by Mut-d3 seemed to be much fuzzy and the plaque size of Mut-p7 had a bigger deviation (Fig. 1B). These results indicated that no unique cysteine is crucial for virus survival but some cysteines may play more important role in the function of the S protein.

Multiple cysteines in the S endodomain were concurrently responsible for virus replication

Previous studies have shown that when the CR motif of the S protein was mostly deleted (leaving only four or five cysteines), the production of recombinant MHVs was not affected, but the cell–cell fusion was decreased dramatically (Yang et al., 2011; Ye et al., 2004). To determine the exact number of cysteines required for the

survival of MHV, mutant viruses with only one to six cysteines left in the CR motif of S gene were constructed (Fig. 2A). Meanwhile, in order to facilitate the detection of viral survival, gene 4 was replaced by an EGFP reporter in these mutants (Fig. 2A). L2 cells were infected with supernatants of the various mutant MHVs produced by targeted RNA recombination and visualised by microscopy at 24 h post infection (hpi). The recombinant MHVs containing one to four cysteine residues in the motif (MH54GFP-1C to -4C) failed to induce any visible syncytia, and the recombinant MHVs with five or six cysteine residues in the motif (MH54GFP-5C and -6C) induced only light syncytia formation (Fig. 2B). Fluorescent microscopy showed that the MH54GFP-1C and -2C mutant viruses failed to express EGFP, that the MH54EGFP-3C virus expressed a low level of EGFP, and that the MH54GFP-4C, -5C and -6C mutants expressed a high level of EGFP (Fig. 2C). These results indicated that the replication of the virus depends on the number of cysteine residues in the CR motif and that at least three cysteines in the motif are required for the viability of the recombinant MHVs.

Deletion of the cysteine-rich motif impaired the localisation of the S protein to the cell surface

The substitution of the cytoplasmic tail of the MHV S protein, which contains the CR motif, with the cytoplasmic tail of the VSV G protein resulted in abolition of cell–cell fusion but did not interfere with expression of the S protein on the cell surface (Bos et al., 1995). The replication of coronaviruses is critically affected by the cellular localisation of the S protein. The less S protein that is expressed on the cell surface, the weaker the extent of cell–cell fusion (Bosch et al., 2003). We previously found that membrane-anchored HK protein and cytoplasmic EGFP were differentially located within the cell (Yang et al., 2011).

In this study, the distribution of the HK proteins expressed by four recombinant MHVs (Fig. 3A) was further explored by sequential staining to the living and permeabilized cells with two anti-HA antibodies. Two HK proteins, the HKM protein with wild-type MHV S Tm/Endo and the HKP protein with a Tm and a truncated Endo of platelet-derived growth factor receptor (PDGFR) without cysteine residues, were largely localised on the cellular surface (upper two panels in Fig. 3B). However, HK-2C and HK-6C with the MHV S Tm but partially deleted CR in the Endo were found to be principally distributed in the cytoplasm (bottom two panels in Fig. 3B). These results indicated that the sequence containing charged residues rather than the number of cysteines in the motif is essential for the accumulation of S protein on the plasma membrane.

Multiple cysteines in the endodomain enhance the incorporation of S protein to DRMs

DRMs are membrane subdomains that are resistant to solubilisation with cold non-ionic detergents, such as Triton X-100 (Lingwood and Simons, 2007). The extractability of infected Neuro-2a cells was examined by treatment with 1% Triton X-100 in cold TNE buffer. DRMs were separated by flotation ultracentrifugation. All of four HK proteins were distributed in the higher density fractions (fractions 7 to 10) (Fig. 4). Both HKM and HK-6C were also found to diffuse into the lower density fractions (fractions 3 to 4), where the DRM maker protein caveolin-1 was distributed. However, the distribution of HKP and HK-2C to the lower density fractions was significantly reduced (Fig. 4). These results showed that the HK proteins with the wild type CR motif and the CR motif mutant containing only six cysteines were associated with lipid rafts to a higher degree than those recombinant proteins with CR motifs with zero or two cysteines.

Multiple cysteines in the endodomain enhance the S-palmitoylation of the S protein

S-palmitoylation of the MHV S protein has been shown to focus on the carboxyl terminal cysteine residues and is necessary for virus assembly (Bosch et al., 2005; Thorp et al., 2006). The S-palmitoylation of some membrane-proximal cysteine clusters in the SARS CoV S protein may be important for S-mediated cell fusion, and it may also be necessary for the partitioning of the S protein into DRMs (McBride and Machamer, 2010; Petit et al., 2007). Hydroxylamine treatment (Drisdel et al., 2006; Gonzalo and Linder, 1998; Valdez-Taubas and Pelham, 2005) has been used to detect the S-palmitoylation level of HK proteins expressed by recombinant MHVs in Neuro-2a cells (Fig. 5A). The electrophoretic mobility of HK proteins was examined after treatment with or without hydroxylamine. The mobility of the HKM and HK-6C proteins was significantly altered, whereas that of the HK-2C and HKP mutants was not (Fig. 5B). These results indicated that the level of S-palmitoylation is correlated with the number of cysteine residues in the CR motif of the S protein endodomain. Moreover, the level of S-palmitoylation is consistent not only with the survival of the recombinant MHV (Fig. 2) but also with the association of S protein in lipid rafts of the infected cells (Fig. 4).

Discussion

Both the Tm and the Endo of the S protein are essential for virion assembly and membrane fusion of coronaviruses (Bos et al., 1995; Bosch et al., 2005; Chang et al., 2000; Petit et al., 2007; Shulla and Gallagher, 2009; Thorp et al., 2006; Ye et al., 2004). The Tm is an efficient membrane anchor because of its integration of hydrophobic residues with lipids of membranes. Some charged residues of the Endo have been shown to direct the S protein to specifically assemble into virions via their interactions with membranes or other structural proteins (Bosch et al., 2005; Ye et al., 2004). The cysteines in the Endo have been shown to enhance the trafficking and membrane binding of S proteins to cells through the S-palmitoylation of the S proteins (Bos et al., 1995; McBride and Machamer, 2010; Petit et al., 2007; Thorp et al., 2006).

To analyse the effects of the cysteine residues in the unique CR motif on the replication of murine coronavirus, two sets of recombinant MHVs were generated by targeted RNA recombination (Masters, and Rottier, 2005; Masters et al., 2006). One set, in which substitution or deletion mutations of the CR were directly located in the S protein Endo, was constructed to determine the survival and plaque morphology of recombinant MHVs in mouse L2 cells (Figs. 1 and 2). The other set of recombinant MHVs was comprised of the S gene and the replacement of the hemagglutinin–esterase gene with a foreign Hook gene (Masters et al., 2006; Ye et al., 2004). These recombinant viruses were able to infect mouse Neuro-2a cells and express the recombinant HK proteins (Yang et al., 2011). The HA-tagged non-viral scFv Ecto of HK served as a surrogate for the S protein Ecto and was designed to eliminate possible interference of the cysteine residues in the S protein ectodomain. The HK proteins with four types of Tm/Endo combinations, constructed from wild type protein, mutated MHV S protein (HKM, HK-2C and -6C) and truncated PDGFR (HKP), were used to analyse the membrane-associated functions (Figs. 3 to 5). In addition, the non-essential gene 4 of MHV was replaced with the reporter gene EGFP in some recombinant MHVs (Das Sarma et al., 2002; Hurst et al., 2005; Yang et al., 2011) (Figs. 2C and 3B).

Previous studies have shown that the CR motif of the S protein Endo is associated with the ability of the S protein to induce syncytia (Bos et al., 1995; Bosch et al., 2005; Chang et al., 2000; Thorp et al., 2006; Ye et al., 2004). In this study, the cysteines in the CR motif were mutated either alone or in combination with alanine, glycine, or serine, and no specific cysteine was found to be crucial for the survival of the recombinant MHVs (Fig. 1). The difference in the plaque morphology among these survived mutants implied that some cysteines may play more important roles in viral replication. We found that the plaques of Mut-p7 and Mut-d3 were uneven and slightly smaller than those of Mut-p2 and -p3, but the plaques of Mut-p6 were slightly larger than those of the other mutants (Figs. 1B and C). The two cysteines in this region were more important for the incorporation of S proteins into virions, which consolidated previous results (Shulla and Gallagher, 2009; Ye et al., 2004). On the other hand, the deletion of the CR motif (Mut-d1), the partial deletion of the motif near the Tm (Mut-d2), and the mutation of all nine cysteines to alanines (Mut-p1) were lethal for the recombinant MHVs, which indicated that six cysteines close to the Tm might be critical for survival of recombinant viruses (Fig. 1B). Further, three cysteines in centre of CR motif (Mut-3 and Mut-4) might play more important role in viral replication (Figs. 1B and C).

Based on the above results, we hypothesise that the multiple cysteines in the motif may account for the function of S proteins. To verify this hypothesis, some deletion mutations of the motif retained one to six cysteines were introduced into recombinant MHVs in which the EGFP reporter gene was substituted for gene 4 (Fig. 2A). These results indicated that only the recombinant MHVs with three or more cysteines were viable (Fig. 2C). However, the ability to induce syncytia by the recombinant MHVs with only three to six cysteines in S protein CR motif was dramatically decreased in L2 cells (Fig. 2B). The decreased CPE was consistent with results of previous studies (Yang et al., 2011; Ye et al., 2004).

The subcellular distribution of recombinant HK proteins in infected Neuro-2a cells provided an explanation for this phenomenon. The distribution of the wild type S Endo (HKM) or PDGFR Endo (HKP) mutants was in the plasma membrane and on the cell surface. However, the mutants with truncated CR motifs (HK-2C and -6C) were distributed in the cytoplasm (Fig. 3). This redistribution of recombinant proteins might be attributed to the deletion of some of the positively charged residues other than the cysteines in the motif. The charged residues, located on the cytoplasmic tail of transmembrane proteins, generally serve as the trafficking and sorting signals to different membrane compartments, including the plasma membrane (Itin et al., 1995). Further investigation of the charged residues in the CR motif of the MHV S will be needed to address this issue.

The number of cysteines in the CR motif of the MHV S protein was shown to directly correlate with its trafficking to lipid rafts of the cell membrane (Fig. 4), and the correlation is also consistent with the levels of S-palmitoylation of the recombinant HK proteins (Fig. 5). The recombinant proteins with either a wild-type CR motif (HKM) or a CR motif containing six cysteines (HK-6C) could be S-palmitoylated and incorporated into DRMs. The mutants with either two cysteines (HK-2C) or no cysteines (HKP) in the CR motif could neither be S-palmitoylated nor be incorporated into DRMs.

Three 3-cysteine clusters in the motif might guarantee the S-palmitoylation, which is beneficial to the association of the S protein to the lipid rafts during viral membrane fusion and virion assembly (Fig. 6). Both trafficking between membranes signalized by the
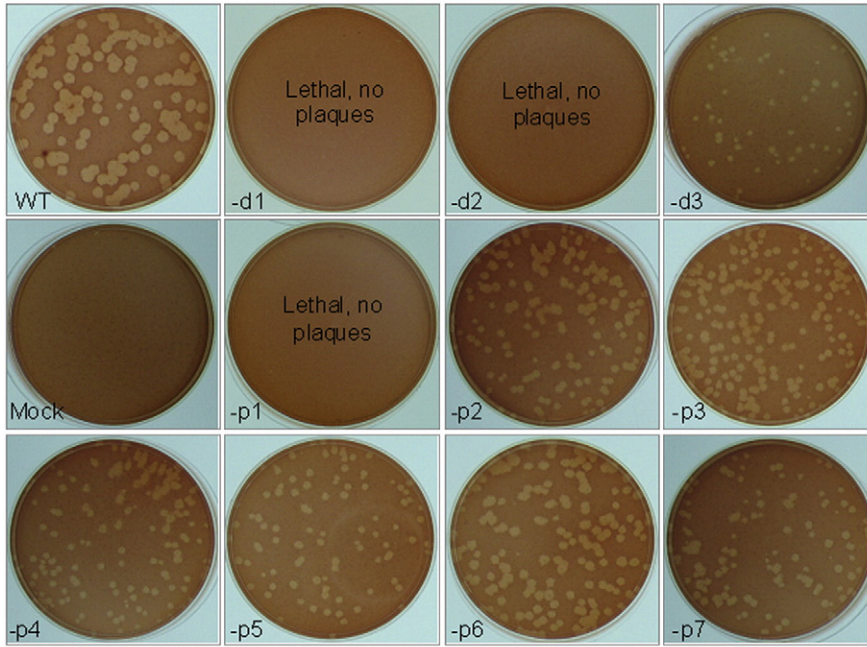
Fig. 1. *Effects of the mutations in the cysteine-rich motif of the S protein endodomain on the production of recombinant MHVs.* (A) The diagram represents part of the genomic organisation of MHV A59 in which the mutated region in the S gene is marked with a full triangle (▲). Sequence alignment of the MHV S transmembrane domain and endodomain shows the deleted amino acid residues (Mut-d1 to -d3) and site-mutated cysteine residues (Mut-p1 to -p7) in the cysteine-rich motif. The sequence of MHV WT is from the wild-type MHV A59 S protein. (B) Comparison of the plaque morphology on the L2 monolayers produced by the recombinant MHVs with a series of mutations in the cysteine-rich motif. 'Lethal, no plaques' indicates the mutation is lethal and no recombinant virus production by the RNA targeted recombination; 'mock' indicates the infection with virus-free medium. (C) Comparison of the plaque size of wild type and the recombinant MHVs. Plaque diameter was gauged by the enlarged photographs of plaques with computer plotter and sized in millimetre (mm). Data are expressed as the mean value and the standard deviation of each survived mutant. t value and $p < 0.001$ (***) , relative to the wild type.
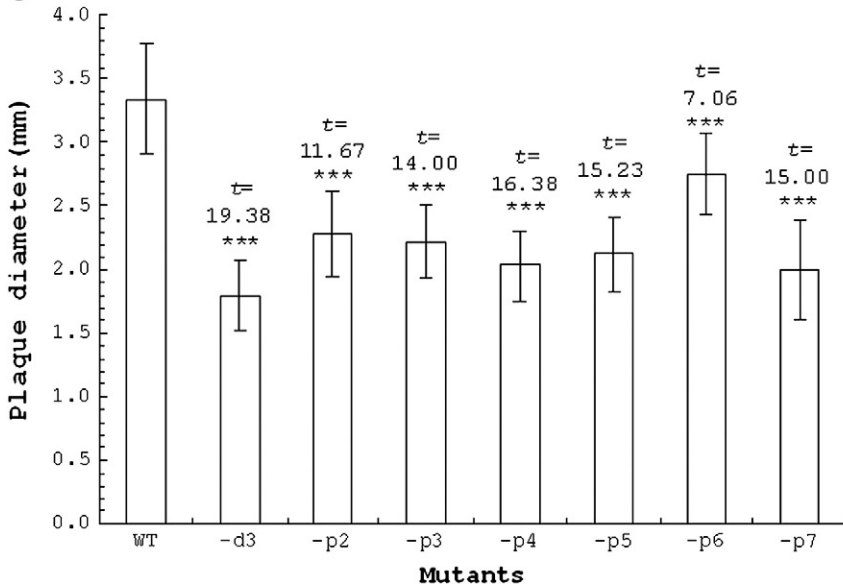
A
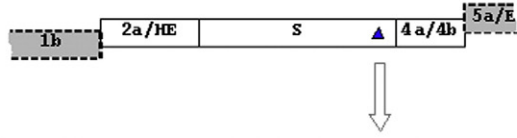
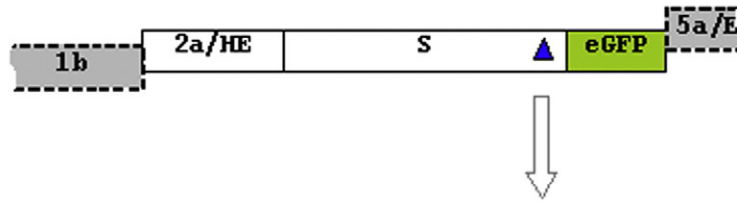| Mutations in S	Transmembrane Domain Endodomain
MHV WT	-EMYVK**WPWYVW**LLIGLAGVAVCVLLFFI<u>CCC</u>TG<u>C</u>GS<u>CC</u>FKK<u>C</u>GN<u>CC</u>DEYGGHQDSIVIHNISSHED
Mut-d1	-EMYVK**WPWYVW**LLIGLAGVAVCVLLFFI------------------DEYGGHQDSIVIHNISSHED
Mut-d2	-EMYVK**WPWYVW**LLIGLAGVAVCVLLFFI----------FKKCGNCCDEYGGHQDSIVIHNISSHED
Mut-d3	-EMYVK**WPWYVW**LLIGLAGVAVCVLLFFICCCTGCGSCCF------DEYGGHQDSIVIHNISSHED
Mut-p1	-EMYVK**WPWYVW**LLIGLAGVAVCVLLFFI<u>AAA</u>TG<u>A</u>GS<u>AA</u>FKK<u>A</u>GN<u>AA</u>DEYGGHQDSIVIHNISSHED
Mut-p2	-EMYVK**WPWYVW**LLIGLAGVAVCVLLFFI<u>A</u>CCTGCGSCCFKKCGNCCDEYGGHQDSIVIHNISSHED
Mut-p3	-EMYVK**WPWYVW**LLIGLAGVAVCVLLFFIC<u>SA</u>TGCGSCCFKKCGNCCDEYGGHQDSIVIHNISSHED
Mut-p4	-EMYVK**WPWYVW**LLIGLAGVAVCVLLFFICCCTG<u>A</u>GSCCFKKCGNCCDEYGGHQDSIVIHNISSHED
Mut-p5	-EMYVK**WPWYVW**LLIGLAGVAVCVLLFFICCCTGCGS<u>AA</u>FKKCGNCCDEYGGHQDSIVIHNISSHED
Mut-p6	-EMYVK**WPWYVW**LLIGLAGVAVCVLLFFICCCTGCGSCCFKK<u>A</u>GNCCDEYGGHQDSIVIHNISSHED
Mut-p7	-EMYVK**WPWYVW**LLIGLAGVAVCVLLFFICCCTGCGSCCFKKCGN<u>GS</u>DEYGGHQDSIVIHNISSHED

B

C

A

| Mutations in S	Transmembrane Domain	Endodomain
MHV WT	-EMYVKWPWYVWLLIGLAGVAVCVLLFFI<u>CCC</u>TG<u>C</u>GS<u>CC</u>FKK<u>C</u>GN<u>CC</u>DEYGGHQDSIVIHNISSHED
Mut-1C	-EMYVKWPWYVWLLIGLAGVAVCVLLFFI<u>C</u>----------------DEYGGHQDSIVIHNISSHED
Mut-2C	-EMYVKWPWYVWLLIGLAGVAVCVLLFFI<u>CC</u>--------------DEYGGHQDSIVIHNISSHED
Mut-3C	-EMYVKWPWYVWLLIGLAGVAVCVLLFFI<u>CCC</u>-------------DEYGGHQDSIVIHNISSHED
Mut-4C	-EMYVKWPWYVWLLIGLAGVAVCVLLFFI<u>CCCC</u>------------DEYGGHQDSIVIHNISSHED
Mut-5C	-EMYVKWPWYVWLLIGLAGVAVCVLLFFI<u>CCCCC</u>-----------DEYGGHQDSIVIHNISSHED
Mut-6C	-EMYVKWPWYVWLLIGLAGVAVCVLLFFI<u>CCCCCC</u>-----------DEYGGHQDSIVIHNISSHED

B
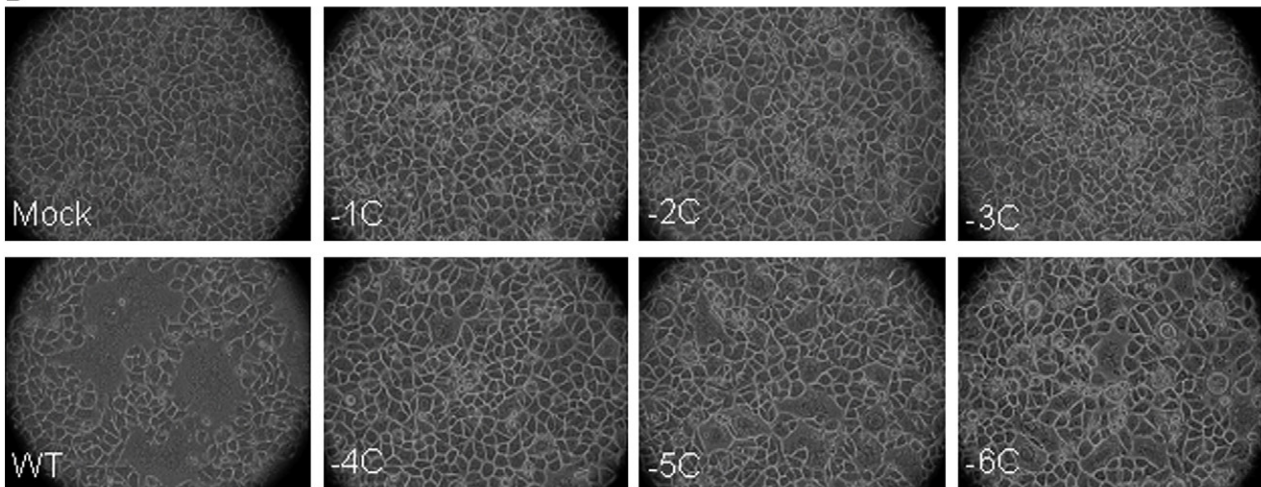
C
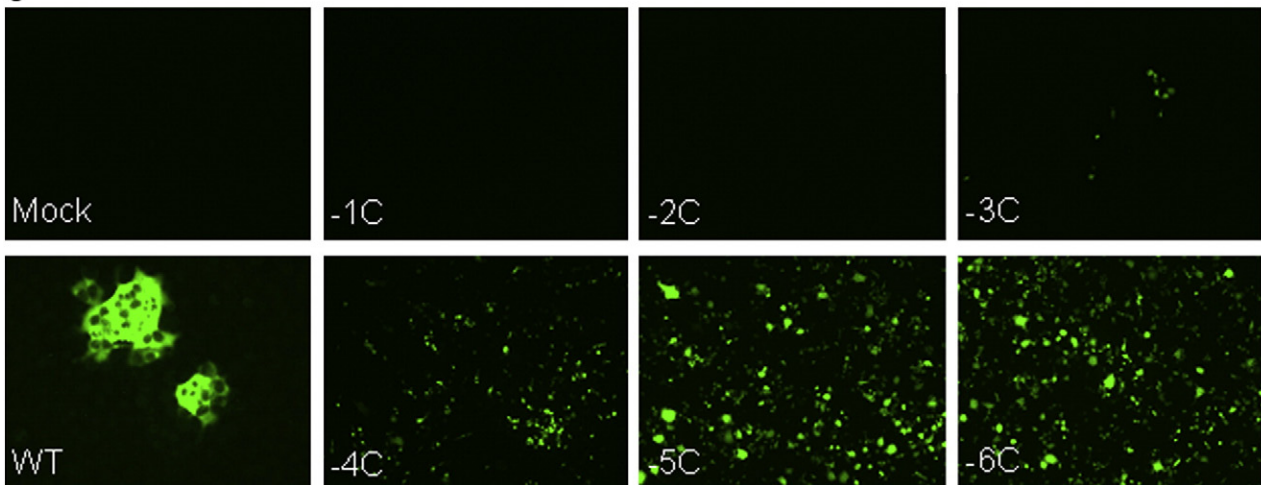
Fig. 2. *Effects of the number of cysteines in the S protein endodomain on the production and cytopathogenesis of recombinant MHVs.* (A) The diagram represents part of the genomic organisation of the EGFP-replaced mutant MH54GFP derived from MHV A59 in which the mutated region in the S gene is marked with a full triangle (▲). The sequence alignment shows the deletion mutations with the numbers of cysteine residues (MH54GFP-1C to -6C) replacing the cysteine-rich motif. (B) L2 cells infected with recombinant MHVs (24 hpi) were visualised under contrast microscope (with magnification 400×) and showed no syncytia (-1C to -4C), small syncytia (-5C and -6C), and large syncytia of wild-type MHV (12 hpi). (C) L2 cells infected with recombinant MHVs (24 hpi) newly produced by RNA-targeted recombination were visualised under fluorescent microscope (with magnification 100×), which showed no cells infected (-1C to -2C), a few cells infected (-3C), more cells infected (-4C to -6C); small syncytia (-5C and -6C) and large syncytia of wild-type MHV (12 hpi).
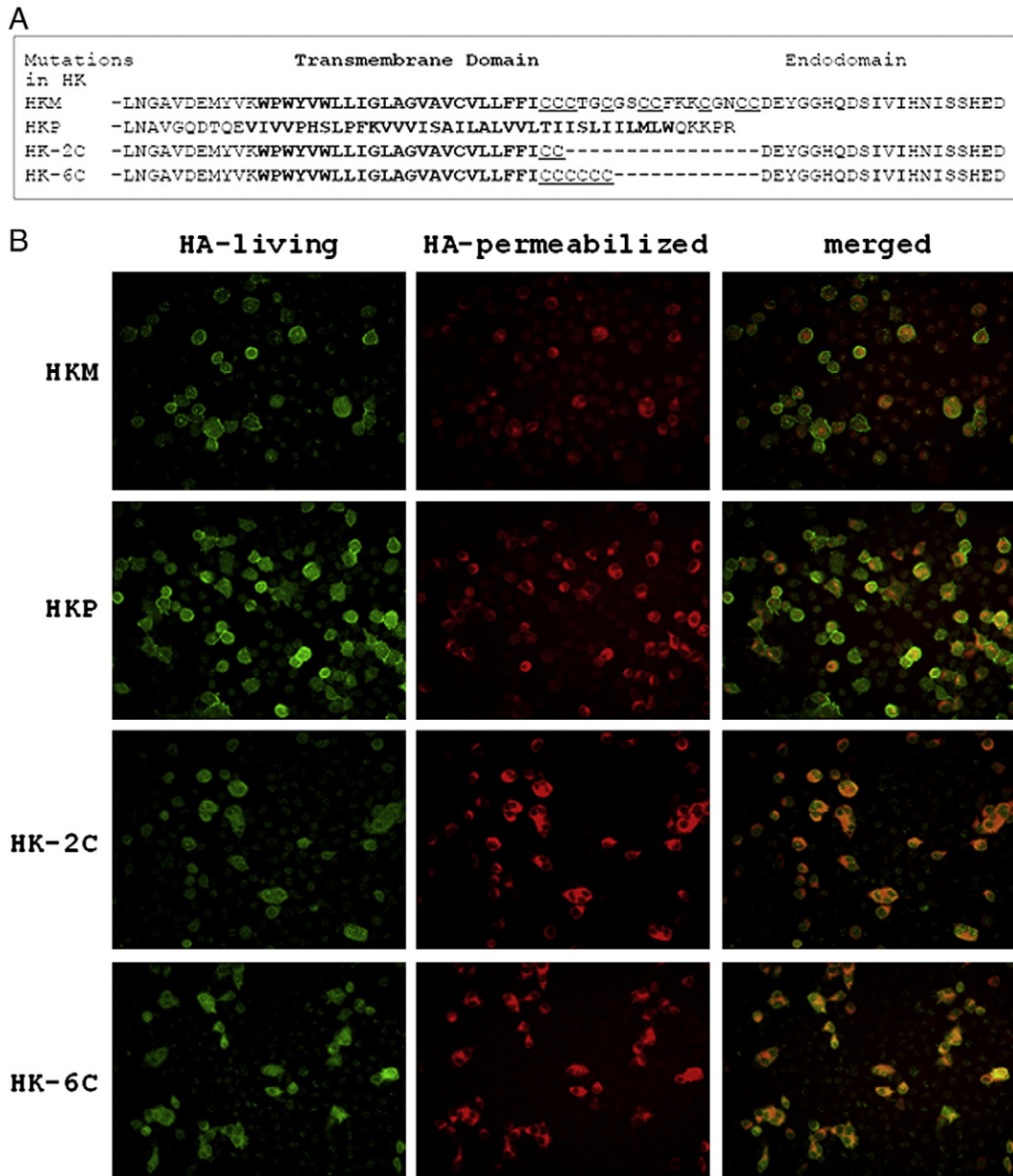
Fig. 3. *Location of HK proteins with different transmembrane domains and/or endodomains on cellular surfaces.* (A) The sequence alignment shows the four combinations of transmembrane domains and endodomains of HK proteins derived from the MHV S protein (HKM, HK-2C, HK-6C) and the PGDFR (HKP). (B) Staining of HKM, HKP, HK-2C, and HK-6C in Neuro-2a cells infected with recombinant MHVs. The green fluorescence indicates the HK proteins on the surfaces of living cells with a rat anti-HA tag antibody and an FITC-labeled secondary antibody. The red fluorescence indicates the HK protein in cytoplasm of permeabilised cells with a mouse anti-HA tag antibody and a TRITC-labeled secondary antibody.

positively charged residues and S-palmitoylation as well as lipid raft incorporation induced by the cysteines residues were primarily uncovered in this study.

Materials and methods

Plasmid construction

The donor RNA transcription vectors used in this study were derived from pMH54, pMH54GFP, pHKM and pHKP (Das Sarma et al., 2002; Kuo et al., 2000; Ye et al., 2004). The construction strategy we used has been previously described (Yang et al., 2011). Briefly, pMH54 and pMH54GFP transcription vectors were digested with MluI and SbfI, and a set of homogenous fragments with point or

deletion mutations in the CR motif were inserted. These fragments were generated by splicing overlap extension-PCR (Aiyar et al., 1996) using pMH54 DNA as a template that contained the endodomain sequence of MHV S gene.

Both pHKM and pHKP were previously constructed (Ye et al., 2004). The recombinant hook protein (HK) gene contained a DNA sequence encoding a signal peptide from the immunoglobulin λlight chain, an HA tagged-scFv ectodomain and a Tm/Endo from either the MHV S gene or a truncated PDGFR gene (Masters et al., 2006; Yang et al., 2011; Ye et al., 2004). For the generation of pHK-2C and pHK-6C, pHKM as the reception vector was digested with SalI and AscI and two homogenous fragments with mutations in the cysteine-rich motif were inserted. All DNA manipulations were performed according to standard molecular cloning procedures (Sambrook and Russell, 2001).
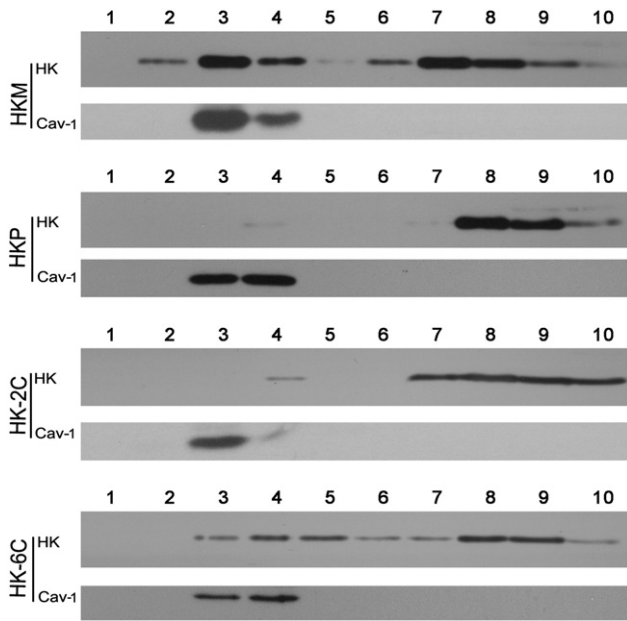
Fig. 4. *Cysteines in the S protein endodomain enhance the incorporation of HK proteins into DRMs of Neuro-2a cells infected with recombinant MHVs.* DRMs were isolated by discontinuous density ultracentrifugation in sucrose from Neuro-2a cells infected with four recombinant MHVs (HKM, HKP, HK-2C, and HK-6C) and ten fractions were collected from low to high density. HK protein (HK, upper panel) and DRM marker caveolin-1 (cav-1, bottom panel) in each fraction were identified by Western blotting with anti-HA and anti-caveolin-1 antibodies respectively. The majority of DRM was located in fractions 3 and 4. HK protein was distributed in several fractions.

All constructs were identified by restriction digest analysis, and all cloning sites and junctions in synthetic plasmids were confirmed by DNA sequencing.

Cell culture and viruses

Mouse neuroblastoma Neuro-2a cells were purchased from the Institute of Cellular Biology, China Academy of Sciences. Neuro-2a cells were maintained in MEM (GIBCO, Invitrogen) supplemented with 5% FBS (Hyclone) and 0.20% sodium bicarbonate (Sigma-Aldrich). Mouse L2 cells, *Felis catus* whole fetus (FCWF) cells, wild-type MHV A59 and the engineered parent virus fMHV stocks were kindly provided by Dr. Paul S. Masters (Wadsworth Center, Albany, New York). L2 and FCWF cells were grown in DMEM (GIBCO, Invitrogen) supplemented with 10% FBS and 0.37% sodium bicarbonate. The cells were cultivated in a humidified 5% CO_2 atmosphere at 37 °C. For infection with MHV
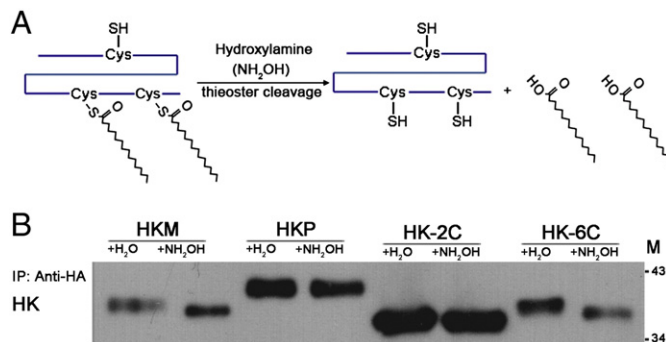

Fig. 5. *Cysteines in the endodomain enhance the S-palmitoylation of HK proteins expressed by recombinant MHVs.* (A) The diagram shows the chemical cleavage of the thioester bonds of S-palmitoylated proteins with hydroxylamine (NH_2OH). (B) The electrophoretic migration of four HK fusion proteins treated with ($+NH_2OH$) or without ($+H_2O$) hydroxylamine was examined by SDS-PAGE (4–20%) and Immunoblotting. M and number indicate the molecular weight (kDa).

or recombinant MHVs, monolayers of cells at 60–80% confluence were inoculated at a multiplicity of infection (MOI) of 0.1–1.0.

Production of recombinant MHVs

Recombinant MHVs were produced according to the procedure of targeted RNA recombination developed by Kuo et al. (2000) and Masters and Rottier (2005). fMHV is a chimeric MHV A59 strain virus in which the ectodomain of the S gene is replaced with that of feline infectious peritonitis virus. This replacement results in the fact that recombinant virus is grown in feline FCWF cells but not in murine L2 cells. Donor RNA transcription vectors were linearised by digestion with PacI and transcribed into mRNAs using the mMESSAGE mMACHINE T7 Ultra kit (Ambion). Approximately 10 μl of each recombinant transcript was prepared for transfection of ~10^7 of FCWF cells. The fMHV-infected cells were briefly digested with a low concentration of trypsin at 2 h post-infection (hpi). RNA transfection was performed using a Gene Pulser XceII electroporation system (Bio-Rad) with one pulse at settings of 975 μF and 0.3 kV. The infected and transfected FCWF cells were then added to 6-well cell-culture clusters seeded with L2 monolayers. Culture supernatants containing recombinant MHVs were collected at 24, 48 and 72 hpi. Recombinant MHVs were plaque-purified twice on L2 cells, and all mutations were verified by RT-PCR and sequencing.

Plaque assay

L2 cells were grown in 60-mm dishes and infected with 1 ml of viruses at dilutions of 10^{-3}, 10^{-4}, 10^{-5} and 10^{-6} for 2 h at 37 °C. Seven milliliters of 0.95% agar (Amresco) in DMEM with 5% FBS was overlaid onto the cells. Plaques were picked at 48 hpi. For visualisation of the plaques, 3 ml of 0.95% agar containing 50 μg/ml neutral red (Sigma-Aldrich) was overlaid onto the plate. Plaques were photographed on a white light transilluminator (Upland) with a digital camera after incubation for 6 to 8 h at 37 °C.

Confocal immunofluorescence

Neuro-2a cells were grown on glass coverslips coated with poly L-lysine (Sigma-Aldrich) to ~60% confluence and then infected with recombinant MHV that expressed HKM, HKP, HK-2C, or HK-6C. At 16–18 hpi, the cells were washed with PBS and incubated with a rat mAb to the HA tag (Roche) for 1 h at 37 °C for staining the HK proteins on the cell surface. Then cells were fixed with 4% paraformaldehyde (Sigma-Aldrich) in PBS for 20 min and permeabilized with 0.1% Triton X-100 (Sigma-Aldrich) in PBS for 5 min at room temperature. Fixed cells were blocked with 3% BSA and then incubated with a mouse mAb to the HA tag (Roche) overnight at 4 °C. The cells were then incubated with a FITC-conjugated antibody to rat IgG and a TRITC-conjugated antibody to mouse IgG (Jackson ImmunoResearch) for 1 h at room temperature. At last the cells were washed three times in PBS and mounted with Mowiol antifade reagent (Sigma-Aldrich). Fluorescent images were obtained using a Leica TCS-SP5 laser-scanning confocal microscope and processed with LAS AF software (Leica).

Analysis of DRM association

DRM fractions were isolated using discontinuous density ultracentrifugation as previously described (Brown and London, 1998; Hooper, 1999; McBride and Machamer, 2010; Zhang et al., 2000). At 12 hpi, Neuro-2a cells were rinsed twice with ice-cold PBS and lysed on ice for 30 min in 1 ml of TNE buffer (10 mM Tris–HCl, 150 mM NaCl and 5 mM EDTA, pH 7.4) containing a protease inhibitor cocktail (Roche) and 1% Triton X-100. After passing through a 25-G needle 10 times, lysates were mixed with 1 ml of 80% (w/v) sucrose in TNE. The

mixture was overlaid with 4 ml of 35% sucrose in TNE and then with 1 ml of 5% sucrose in TNE. Finally, 3 ml of TNE was overlaid on the 5% sucrose solution. After centrifugation for 18 h at 285,000×g at 4 °C (SW40 rotator, Beckman-Coulter), 1.0 ml fractions were collected from the top to bottom of the gradient and analysed by 10% SDS-PAGE and Western blotting with mAbs to the HA tag (Roche) and to caveolin-1 (Abcam).

Hydroxylamine treatment

The levels of S-palmitoylation of recombinant proteins were analysed by a shift in the electrophoretic mobility after treatment with hydroxylamine (Drisdel et al., 2006; Gonzalo and Linder, 1998; Valdez-Taubas and Pelham, 2005). In brief, infected monolayers of Neuro-2a cells were washed twice with ice-cold PBS and dissolved in 300 μl of IPP buffer (50 mM Tris–HCl, 150 mM NaCl, 1.0% Nonidet P-40, pH 8.0) containing a protease inhibitor cocktail. Cell lysates were held on ice for 5 min and then clarified by centrifugation at 12,000×g for 5 min at 4 °C. Clarified lysates were mixed with 15 μl of Anti-HA Affinity Matrix (Roche) by inversion overnight at 4 °C. The matrix was precipitated by centrifuging at 12,000×g for 30 s, and the supernatant was carefully removed. The matrix was washed with 1 ml of cold IPP buffer three times. The final rinsed matrix was suspended in 60 μl of 2× SDS sample buffer and heated at 95 °C for 5 min. The immunoprecipitated proteins were divided into two parts. One was mixed with an equal volume of 2 M hydroxylamine (Sigma-Aldrich) in water at room temperature for 1 h, and the other was mixed with an equal volume of water as a control. The samples were separated by SDS-PAGE with 4–20% gradient gel (Bio-Rad) and characterised by Western blotting using an anti-HA tag mAb (Roche).

Gel electrophoresis and Western blotting

Protein samples were separated by 10% SDS-PAGE and transferred to PVDF membrane using a Mini Trans-blot Electrophoretic Transfer Cell (Bio-Rad) according to the laboratory manual (Sambrook and Russell, 2001). The membranes were blocked with 5% nonfat milk in PBST (PBS containing 0.1% (v/v) Tween-20) for 1 h at room temperature followed by an incubation with a mAb to the HA tag (Roche) overnight at 4 °C. After washing three times in PBST, membranes were incubated with an HRP-conjugated secondary antibody (GE, Amersham) in 5% nonfat milk-PBST for 1 h at room temperature and washed again with PBST. Signals were visualised using the ECL detection system (GE, Amersham) according to the manual instructions.
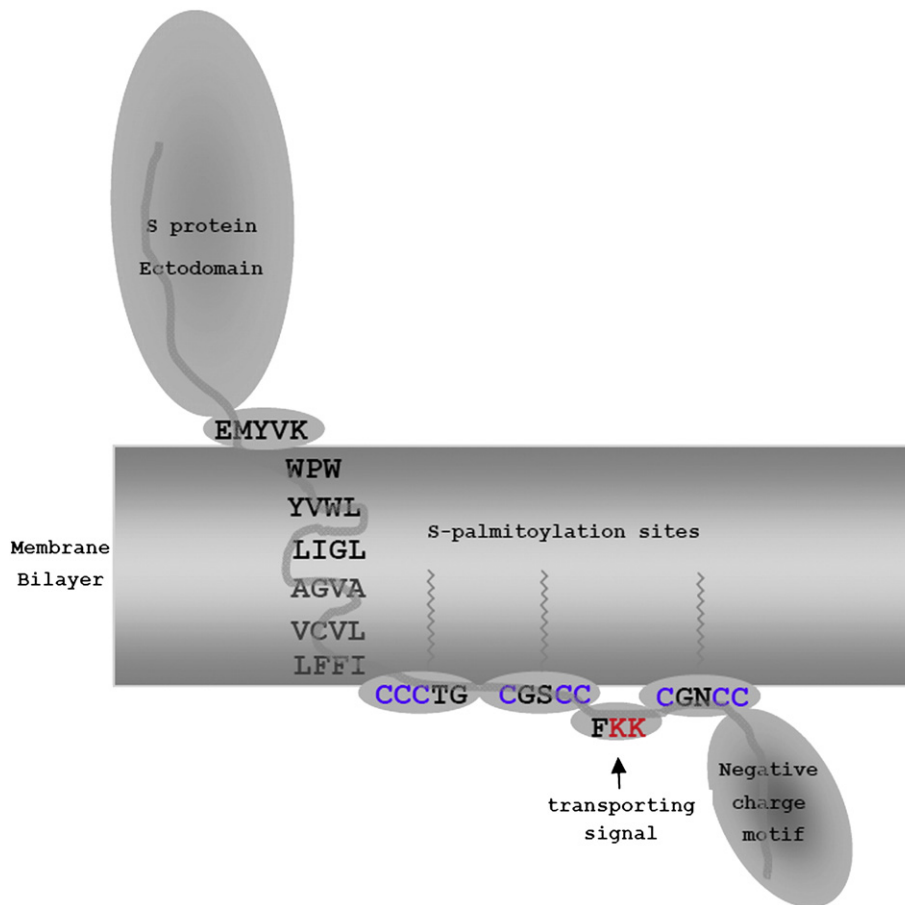
Acknowledgments

Fig. 6. *Functional motifs and S-palmitoylation of the endodomain of mouse coronavirus spike protein.* Residues of transmembrane domain and cys-rich motif were showed in diagram. S-palmitoylation could occur at all cysteines (C, in blue) in the motif, while the primary site may require a residue cluster containing at least three cysteines. The S-palmitoylation would be enhanced by extra cysteines in the motif and lead proteins to incorporate to lipid rafts. Two positive-changed lysine residues (KK, in red) in the motif might serve as a signal for transportation of S protein to cellular surface. The S-palmitoylation at the site between the transportation signal and the terminal cluster of negative-charged residues, a putative motif interaction with M protein of the virus, is crucial for viral assembly and entry.

References

Aiyar, A., Xiang, Y., Leis, J., 1996. Site-directed mutagenesis using overlap extension PCR. Methods Mol. Biol. 57, 177–191.

Bos, E.C., Heijnen, L., Luytjes, W., Spaan, W.J., 1995. Mutational analysis of the murine coronavirus spike protein: effect on cell-to-cell fusion. Virology 214 (2), 453–463.

Bosch, B.J., van der Zee, R., de Haan, C.A., Rottier, P.J., 2003. The coronavirus spike protein is a class I virus fusion protein: structural and functional characterization of the fusion core complex. J. Virol. 77 (16), 8801–8811.

Bosch, B.J., de Haan, C.A.M., Smits, S.L., Rottier, P.J.M., 2005. Spike protein assembly into the coronavirion: exploring the limits of its sequence requirements. Virology 334 (2), 306–318.

Branigan, P.J., Day, N.D., Liu, C., Gutshall, L.L., Melero, J.A., Sarisky, R.T., Del Vecchio, A.M., 2006. The cytoplasmic domain of the F protein of human respiratory syncytial virus is not required for cell fusion. J. Gen. Virol. 87 (2), 395–398.

Brown, D.A., London, E., 1998. Functions of lipid rafts in biological membranes. Annu. Rev. Cell Dev. Biol. 14, 111–136.

Carstens, E.B., Ball, L.A., 2009. Ratification vote on taxonomic proposals to the International Committee on Taxonomy of Viruses (2008). Arch. Virol. 154 (7), 1181–1188.

Chang, K.W., Sheng, Y., Gombold, J.L., 2000. Coronavirus-induced membrane fusion requires the cysteine-rich domain in the spike protein. Virology 269 (1), 212–224.

Chen, B.J., Takeda, M., Lamb, R.A., 2005. Influenza virus hemagglutinin (H3 subtype) requires palmitoylation of its cytoplasmic tail for assembly: M1 proteins of two subtypes differ in their ability to support assembly. J. Virol. 79 (21), 13673–13678.

Das Sarma, J., Scheen, E., Seo, S.H., Koval, M., Weiss, S.R., 2002. Enhanced green fluorescent protein expression may be used to monitor murine coronavirus spread in vitro and in the mouse central nervous system. J. Neurovirol. 8 (5), 381–391.

Drisdel, R.C., Alexander, J.K., Sayeed, A., Green, W.N., 2006. Assays of protein palmitoylation. Methods 40 (2), 127–134.

Gonzalo, S., Linder, M.E., 1998. SNAP-25 palmitoylation and plasma membrane targeting require a functional secretory pathway. Mol. Biol. Cell 9 (3), 585–597.

Holmes, K.V., 2003. SARS-associated coronavirus. N. Engl. J. Med. 348 (20), 1948–1951.

Hooper, N.M., 1999. Detergent-insoluble glycosphingolipid/cholesterol-rich membrane domains, lipid rafts and caveolae. Mol. Membr. Biol. 16 (2), 145–156.

Hurst, K.R., Kuo, L., Koetzner, C.A., Ye, R., Hsue, B., Masters, P.S., 2005. A major determinant for membrane protein interaction localizes to the carboxyterminal domain of the mouse coronavirus nucleocapsid protein. J. Virol. 79 (21), 13285–13297.

Itin, C., Kappeler, F., Linstedt, A.D., Hauri, H.P., 1995. A novel endocytosis signal related to the KKXX ER-retrieval signal. EMBO J. 14 (10), 2250–2256.

Jin, H., Subbarao, K., Bagai, S., Leser, G.P., Murphy, B.R., Lamb, R.A., 1996. Palmitoylation of the influenza virus hemagglutinin (H3) is not essential for virus assembly or infectivity. J. Virol. 70 (3), 1406–1414.

Kordyukova, L.V., Serebryakova, M.V., Baratova, L.A., Veit, M., 2008. S acylation of the hemagglutinin of influenza viruses: mass spectrometry reveals site-specific attachment of stearic acid to a transmembrane cysteine. J. Virol. 82 (18), 9288–9292.

Kuo, L., Godeke, G.J., Raamsman, M.J., Masters, P.S., Rottier, P.J., 2000. Retargeting of coronavirus by substitution of the spike glycoprotein ectodomain: crossing the host cell species barrier. J. Virol. 74 (3), 1393–1406.

Linder, M.E., Deschenes, R.J., 2007. Palmitoylation: policing protein stability and traffic. Nat. Rev. Mol. Cell Biol. 8 (1), 74–84.

Lingwood, D., Simons, K., 2007. Detergent resistance as a tool in membrane research. Nat. Protoc. 2 (9), 2159–2165.

Lopez, L.A., Riffle, A.J., Pike, S.L., Gardner, D., Hogue, B.G., 2008. Importance of conserved cysteine residues in the coronavirus envelope protein. J. Virol. 82 (6), 3000–3010.

Majeau, N., Fromentin, R., Savard, C., Duval, M., Tremblay, M.J., Leclerc, D., 2009. Palmitoylation of hepatitis C virus core protein is important for virion production. J. Biol. Chem. 284 (49), 33915–33925.

Masters, P.S., 2006. The molecular biology of coronaviruses. Adv. Virus Res. 66, 193–292.

Masters, P.S., Rottier, P.J., 2005. Coronavirus reverse genetics by targeted RNA recombination. Curr. Top. Microbiol. Immunol. 287, 133–159.

Masters, P.S., Kuo, L., Ye, R., Hurst, K.R., Koetzner, C.A., Hsue, B., 2006. Genetic and molecular biological analysis of protein–protein interactions in coronavirus assembly. Adv. Exp. Med. Biol. 581 (III), 163–173.

McBride, C.E., Machamer, C.E., 2010. Palmitoylation of SARS-CoV S protein is necessary for partitioning into detergent-resistant membranes and cell–cell fusion but not interaction with M protein. Virology 405 (1), 139–148.

Petit, C.M., Chouljenko, V.N., Iyer, A., Colgrove, R., Farzan, M., Knipe, D.M., Kousoulas, K.G., 2007. Palmitoylation of the cysteine-rich endodomain of the SARS-coronavirus spike glycoprotein is important for spike-mediated cell fusion. Virology 360 (2), 264–274.

Rocks, O., Peyker, A., Kahms, M., Verveer, P.J., Koerner, C., Lumbierres, M., Kuhlmann, J., Waldmann, H., Wittinghofer, A., Bastiaens, P.I., 2005. An acylation cycle regulates localization and activity of palmitoylated Ras isoforms. Science 307 (5716), 1746–1752.

Rousso, I., Mixon, M.B., Chen, B.K., Kim, P.S., 2000. Palmitoylation of the HIV-1 envelope glycoprotein is critical for viral infectivity. Proc. Natl. Acad. Sci. U. S. A. 97 (25), 13523–13525.

Sambrook, J., Russell, D.W., 2001. Molecular Cloning: A Laboratory Manual, 3rd ed. Cold Spring Harbor Laboratory Press, Cold Spring Harbor, N.Y.

Shulla, A., Gallagher, T., 2009. Role of spike protein endodomains in regulating coronavirus entry. J. Biol. Chem. 284 (47), 32725–32734.

Siddell, S.G., 1995. The Coronaviridae. Plenum Press, New York, N.Y.

Smit, J.M., Bittman, R., Wilschut, J., 2001. Deacylation of the transmembrane domains of Sindbis virus envelope glycoproteins E1 and E2 does not affect low-pH-induced viral membrane fusion activity. FEBS Lett. 498 (1), 57–61.

Takeda, M., Leser, G.P., Russell, C.J., Lamb, R.A., 2003. Influenza virus hemagglutinin concentrates in lipid raft microdomains for efficient viral fusion. Proc. Natl. Acad. Sci. U. S. A. 100 (25), 14610–14617.

Thorp, E.B., Boscarino, J.A., Logan, H.L., Goletz, J.T., Gallagher, T.M., 2006. Palmitoylations on murine coronavirus spike proteins are essential for virion assembly and infectivity. J. Virol. 80 (3), 1280–1289.

Valdez-Taubas, J., Pelham, H., 2005. Swf1-dependent palmitoylation of the SNARE Tlg1 prevents its ubiquitination and degradation. EMBO J. 24 (14), 2524–2532.

Weiss, S.R., Navas-Martin, S., 2005. Coronavirus pathogenesis and the emerging pathogen severe acute respiratory syndrome coronavirus. Microbiol. Mol. Biol. Rev. 69 (4), 635–664.

Whitt, M.A., Rose, J.K., 1991. Fatty acid acylation is not required for membrane fusion activity or glycoprotein assembly into VSV virions. Virology 185 (2), 875–878.

Yang, J., Sun, Z., Wang, Y., Lv, J., Qu, D., Ye, R., 2011. Partial deletion in the spike endodomain of mouse hepatitis virus decreases the cytopathic effect but maintains foreign protein expression in infected cells. J. Virol. Methods 172 (1–2), 46–53.

Ye, R., Montalto-Morrison, C., Masters, P.S., 2004. Genetic analysis of determinants for spike glycoprotein assembly into murine coronavirus virions: distinct roles for charge-rich and cysteine-rich regions of the endodomain. J. Virol. 78 (18), 9904–9917.

Zhang, J., Pekosz, A., Lamb, R.A., 2000. Influenza virus assembly and lipid raft microdomains: a role for the cytoplasmic tails of the spike glycoproteins. J. Virol. 74 (10), 4634–4644.

Zhang, S.X., Han, Y., Blissard, G.W., 2003. Palmitoylation of the Autographa californica multicapsid nucleopolyhedrovirus envelope glycoprotein GP64: mapping, functional studies, and lipid rafts. J. Virol. 77 (11), 6265–6273.